

# The Yucatan Channel flow: Observations vs. CLIPPER ATL6 and MERCATOR PAM05 models.

Julio Candela\*, Sorayda Tanahara\*\*, Michel Crepon\*\* and Bernard Barnier\*\*\*

\*CICESE, Mexico, \*\*LODYC, France, \*\*\*LEGI-CNRS, France.

---

J. Candela, Departamento de Oceanografía Física, CICESE, Apdo., Postal 2732, Ensenada, México. [jcandela@cicese.mx](mailto:jcandela@cicese.mx)

S. Tanahara and M. Crepon, LODYC, Université Pierre et Marie Curie, 75005 Paris, France. [tana@lodyc.jussieu.fr](mailto:tana@lodyc.jussieu.fr), [crepon@lodyc.jussieu.fr](mailto:crepon@lodyc.jussieu.fr)

B. Barnier, LEGI-CNRS, BP53, 38041, Grenoble Cédex 9, France. [bernard.barnier@hmg.inpg.fr](mailto:bernard.barnier@hmg.inpg.fr)

Submitted to JGR-Oceans

December, 2002.

## **Abstract**

The statistical properties of the flow structure in the Yucatan Channel's main section based on two years of continuous observations (august/1999-june/2001) are compared with those simulated by the OPA primitive equation model in two different configurations: the ATL6 configuration from the CLIPPER project (the whole Atlantic domain with a  $1/6^\circ$  resolution), and the PAM05 configuration from the MERCATOR project (the North Atlantic domain from  $9^\circ\text{N}$  to  $70^\circ\text{N}$  with  $1/12^\circ$  resolution). While the observed two-year mean transport into the Gulf of Mexico is 23.06 Sv, ATL6 has a 5-year mean of 27.49 Sv and PAM05 a 3-year mean of 29.06 Sv. Apart from this discrepancy in the mean transport both simulations are able to reproduce well, in structure and magnitude, details of the mean current and its variability. Features like the Yucatan Current core and the deep countercurrents in the Yucatan and Cuban sides are both well reproduced, as well as the presence of a minimum surface current variability at the center of the channel. The two principal empirical modes of current variability, which are related to the passage of eddies through the channel, are also reproduced by the simulations. The observed transports above and below the  $6^\circ\text{C}$  isotherm show no coherency at any frequency, while in both simulations a significant peak of coherence is present at a period around 20 days, which we interpret as a first baroclinic Kelvin mode between the two layers. The observed 2-year mean transport below  $\sim 7^\circ\text{C}$  into the Gulf of Mexico is zero, while both ATL6 and PAM05 simulations have mean transports of  $\sim 0.5$  Sv into the Gulf that are not completely compensated by outflow through the Florida Straits. This implies that a significant vertical mixing occurs in the modeled Gulf of Mexico that needs to be verified in reality. As in the observations the shedding of eddies by the Loop Current in the simulations is preceded by periods of diminished negative horizontal vorticity flux into the Gulf of Mexico. *INDEX TERMS*: 4255 Oceanography: General: Numerical modeling; 4576 Oceanography: Physical: Western boundary currents; 4520 Oceanography: Physical: Eddies and mesoscale processes; 4243 Oceanography: General: Marginal and semienclosed seas.

## **1 Introduction**

The flow through the Yucatan Channel is an integral part of the North Atlantic Ocean Subtropical Gyre circulation with an important contribution from the inter-hemispheric Meridional Overturning Cell (*Schmitz and McCartney, 1993*). The Yucatan Channel is the dynamically relevant entrance of the Gyre's through flow in the Gulf of Mexico, where it gives origin to the Loop Current, and upon exiting the Gulf, to the Florida and Gulf Stream Currents (*Mooers and Maul, 1998*). In recent years the Yucatan Channel and its adjacent regions have been the subject of intensive observational (*Sheinbaum et al, 2002*) and numerical studies (*Murphy et al, 1998; Barnier et al, 2001; Johns et al, 2002; Ezer et al, 2002; Sheng and Tang, 2002*). An evident aspect of the upper layer current patterns in the Caribbean Sea, both observed (*Andrade and Barton, 2001*) and modeled (*op cit*), is the ubiquitous presence of meso-scale eddies passing through the region advected by the mean current flow (dominantly north-westward). There is evidence that a large part of these eddies originate in the equatorial region at the retroflexion of the North Brazil Current, make their way northwestward and, some of them, manage to pass through the gaps between the Lesser Antilles into the Caribbean. Once inside the Caribbean they reformed and continue their way towards the Yucatan Channel where they seem to influence significantly the observed current structure and variability.

Models are important tools for investigating and understanding the ocean dynamics of a given region. However, before a model is used for these purposes, a certain confidence has to be obtained by proving that the model resembles reality and is reproducing the major observed dynamical features. The objective of this work is precisely to build that confidence by looking in detail at how the OPA model (*Madec et al., 1999*), in the CLIPPER ATL6 and MERCATOR PAM05 configurations, reproduces some of the statistical properties of the flow observed in the Yucatan Channel, as well as other implied aspects of the circulation in the region near the Channel. An interesting feature of the model configurations used here is that their domain covers large parts of the Atlantic Ocean and they were not particularly tuned to reproduce well the dynamics of a specific region within the domain. Therefore their behavior in the Yucatan Channel

region, if proved reliable, speaks highly of their overall characteristics as tools to study the dynamics of different regions within the domain.

The paper is organized as follows: After a description of the available observations, the characteristics of the ATL6 and PAM05 model configurations are described, followed by a detailed comparison of the observed and simulated current and transport structure in the Yucatan Channel. At the end the main findings are discussed and summarized.

## **2 Observations during the Canek Program.**

The Canek observing program in the Yucatan Channel region started in December 1996 (*Sheinbaum, et al, 2002*). Up to now there have been 8 cruises in the region dedicated to obtaining hydrographic, bathymetric and moored measurements. During the period between August 1999 and June 2001, an intensive array of moored instruments was deployed in the Yucatan Channel's main section. The objective of this array was to have, for the first time, a detailed measure of the exchange between the Caribbean Sea and the Gulf of Mexico. The array consisted of 8 moorings across the channel's main section between Contoy Island on the Yucatan side, and Cabo San Antonio in Cuba. The moorings were equipped with acoustic current profilers (ADCPs) at the top to measure the surface layers, and up to 7 standard current meters and thermometers below to measure currents and temperature time series at specific depths to monitored the cores of the known water masses in the channel (*Ochoa et al, 2001*). The array was serviced in June 2000 with only minor changes to the original display of instruments. The 23-month long transport measurements thus obtained with this array will be used to compare with the simulations from CLIPPER ATL6 and MERCATOR PAM05. From the Canek cruises there are available 18 complete CTD sections across the channel, done at different times of the year as indicated in Table I. These will be used to compare with the models temperature and salinity structure of variability in the section.

### **3 The Numerical Models.**

#### *CLIPPER ATL6.*

The CLIPPER Project's ATL6 configuration (see the CLIPPER Project ATL6 report on the web for details) is based on the OPA 8.1 primitive equation parallel model (*Madec et al., 1999*). The model domain encompasses the whole Atlantic Ocean from 98° W to 30° E in longitude and 75° S to 70° N in latitude, with a horizontal isotropic 1/6° Mercator grid. Resolution thus decreases from ~5 km at high latitude (the Weddell and Labrador Seas) to 18.5 km at the equator. In the Yucatan Channel the grid resolution is about 17 km. The vertical z-level grid has 43 levels for temperature, salinity and velocity points, with an analytical stretching for finer resolution at the surface. The bottom topography is derived from the bathymetry of *Smith and Sandwell (1997)* and from the Terrainbase 5 dataset south of 72° S, bilinearly interpolated to the model grid with a slight smoothing and a careful check of key passages. The rigid lid assumption and a turbulent kinetic energy mixing scheme with a closure order of 1.5 are used. The model uses a "free slip" lateral boundary condition and a quadratic bottom drag. There are 4 open boundaries where specific transports are specified; these are in the Southern Ocean at 68° W Drake Passage, at 30° E south of Africa, at 8° W in the Gulf of Cadiz, and at 70° N in the Nordic Seas (for details on these open boundaries see *Treguier et al., 2001*). The initial conditions are those of Reynaud et al. (1998) climatology. The model was spun-up for 8 years. For that period it was driven by the 15-year climatology of daily air-sea fluxes from the ECMWF reanalysis project (ERA15, *Gibson et al., 1997*) smoothed with a ten day running average. Then, the model was integrated between 1979 and 1993 using the daily forcing fields from ERA15 interpolated at every time-step. In this particular daily-forced model simulation, ATL6 developed a problem in the Gulf of Mexico after the sixth year of simulation (in 1984) that consisted in a blocking of the Loop Current (i.e. it stopped shedding eddies). The particular reason for this model behavior has not been clarified, but after the last eddy release in October 1983 an anti-cyclonic eddy stationed itself to the north of the Yucatan Channel and remained there for the rest of the simulation until the end of 1993. Because of this anomalous model behavior, only the first 5 years (1979-1983) of the model simulations will be used here.

#### *MERCATOR PAM05.*

The MERCATOR project's "Prototype Atlantique Méditerranée" (PAM) configuration is also based on the OPA 8.1 primitive equation code with z-level coordinates (43 levels). As for the CLIPPER configuration, a "free slip" boundary condition, a rigid lid assumption and turbulent kinetic energy mixing scheme with a closure order of 1.5 are used. The domain covers the North Atlantic Ocean from 9°N to 70°N including the Mediterranean Sea with a 1/12° horizontal resolution. In the Yucatan Channel the horizontal grid spacing is about 7 km. The bathymetry is also interpolated from the Smith and Sandwell (1997) data, with a careful check on key passages. Buffer zones are defined in the southern and northwestern closed boundaries where temperature and salinity are relaxed to seasonal climatological values. These imposed a relatively weak thermohaline circulation ([www.mercator.com.fr](http://www.mercator.com.fr), newsletter 5). After and 11-year spin-up driven with a 3-year mean climatology (1999 to 2001), an inter-annual simulation was carried out with daily forcing using ECMWF analysis air-sea flux products for those 3 years. This latter inter-annual simulation is the one discussed here. An interesting aspect of the PAM05 configuration, in comparison of the ATL6 one, is that it does not include the equatorial variability originating in the North Brazil Current retroflexion region. Also when using the PAM05 simulations to investigate the Caribbean circulation one should keep in mind the proximity of the models' southern open boundary at 9°N.

#### **4 Observations vs. simulations.**

Since the observation time period and the ATL6 simulation are not simultaneous, the observations vs. model comparisons will be made based on their statistical properties. In the case of the PAM05 simulations, besides comparing its statistics, it is also possible to do a more detailed comparison for the time period when they overlap with the observations. The measured time series of hourly currents collected by the instruments at the 8-mooring array (see Fig. 1 for the location of the array), were low-passed with a Lanczos filter with a cut-off period of two days. This filtering procedure effectively eliminates tidal and inertial motions since the inertial period at the channel's latitude is 32 hours. Then the low-passed series were objectively interpolated to obtain maps of along-

channel currents in the Yucatan Channel main section. A six parameter objective mapping, as described in *Ochoa et al.* (2001), was used in which one pair of length scales, 400 m in the vertical and 70 km in the horizontal, describes the ‘small’ scale variability and another pair, 1500 m and 150 km, describes the ‘large’ scale, or background, variability. Two additional parameters, equal to 0.1 and 0.05, describe the noise variance for each scale respectively.

To compare with the observations, data from the two model simulations were extracted along the Yucatan Channel section shown in Figure 1. A similar extraction was performed at a section in the Florida Straits (Figure 1) that will also be discussed later. In the case of the model data the section is sampled regularly at each grid point and no objective interpolation is performed. However, for the Yucatan Channel, due to the fact that the CANEK section does not lie exactly along a constant longitude line, two different extractions were made in the models. In order to get along-channel current across the strait line joining the two channel sides, and because the  $u$  (zonal) and  $v$  (meridional) current components are not sampled at the same grid points (OPA uses a C-grid), an interpolation was needed to sample  $u$ ,  $v$ , temperature and salinity at regularly spaced points along this line. The interpolation scheme followed for each variable was a weighted mean, weighted by the inverse distance to the four closest grid points, to the interpolated point along the section line. This first extraction was used to compare the models current structure and variability with those of the observations. However, due to the interpolation there is a small discrepancy in the mean volume conservation when compared with the transports calculated in the section in the Florida Strait (which is exactly meridional). In the case of the CLIPPER ATL6 simulation, the five-year mean difference in total transports between the sections in Yucatan and Florida is less than 0.3%. In the PAM05 simulation the effect of the interpolation in the 3-year transport difference is 3%. To avoid this lack of volume conservation and to obtain the exact transport calculated by each simulation, a second extraction was performed following exactly the model’s grid (following the stair-case grid geometry). With model data extracted along the grid, and because the “rigid lid” assumption in both model configurations, the matching between simultaneous transports in the Yucatan and Florida

sections is exact. However, since such a procedure extract only  $u$  or  $v$  velocities according to the orientation of the grid, the resulting profile is extremely noisy and cannot be used to study cross section velocity profiles. Therefore, in what follows, this second extraction is the one used whenever cumulative transports are discussed, while the first interpolated extraction is more suitable and used when discussing the current structure in the channel's section.

#### *Current structure.*

Figure 2 shows the along-channel current mean and variability structures from 2 years (Aug. 1999 to June 2001) of observations, 5 years (1979-1983) of ATL6 simulations and 3 years (1999 to 2001) of PAM05 simulations. The observed mean pattern (left upper panel) is characterized by the strong Yucatan Current in the upper western part of the section with surface currents larger than 1 m/s and extending to a depth close to 800 m where the magnitude of the mean current is around 0.1 m/s. This feature is well reproduced by both model simulations' mean structure (central and right upper panels). The simulations also reproduce the observed counter currents at depth at the Yucatan and Cuban sides of the channel, as well as, the presence of the Cuban counter current at the surface. Although this latter feature lacks the isolated character it has in the observations, where it stands as a surface intensified current towards the Caribbean, reaching about 300 meters in depth, and separated from deep Cuban counter flow by a 400 meter thick weak flow towards the Gulf of Mexico. Also well reproduced by both simulations is the persistent, although weak flow, towards the Gulf of Mexico at the central deepest part of the channel section. However, there is an important discrepancy in the mean magnitude of the transport between the observations and the simulations. For the 2 years of observations the total mean transport across the section is 23.06 Sv, whereas it is 27.49 Sv for the 5 years of the ATL6 simulation and is 29.06 Sv for the 3 years of the PAM05 simulation. The observed current variability, expressed as the standard deviation of the observed along-channel current (left lower panel), is characterized by maximum variability at the surface, intensified towards both sides of the channel, with a relative minimum towards the center. At depth, below 800 meters, the magnitude of the current standard deviation is comparable to the mean, an aspect of the

current mean flow that has to do with the fact that waters entering the Gulf below this depth are most likely to leave the Gulf also through Yucatan Channel, since the exit of the Gulf in the Strait of Florida is shallower than 800 meters. Remarkably the standard deviation of the along channel current for both simulations (central and right lower panels) reproduce, reasonably well, all these observed features of the variability, both in structure and magnitude.

A more detailed description of the variability with respect to the mean of the along-channel flow can be obtained by analyzing its empirical mode structure (EOF) (Abascal et al, 2003). Figure 3 shows the first two empirical modes of the observed along-channel current, which together represent around 54% variability. The first mode, which explains 31.3% of the variability, exhibits a surface intensified tripolar structure with coherent currents at both sides of the channel with respect to opposing currents in the center. The second mode, which explains 22.8% of the variability, has a bipolar structure that extends much deeper than for the first mode. Thus it could be related to the passage of eddies which occupy most of the channel's width. These eddies (or current anomalies) can be of either sign, as the time evolution of the mode indicates, and have a clear signature up to 1200 meters depth. In both model simulations the along channel current has an EOF decomposition that resembles well that of the observations as can be seen in Figures 4 and 5. In ATL6 the first mode corresponds to a bipolar mode explaining 59.3% of the variability, while the second mode has a tripolar structure and explains only 19.3% of the variability (Figure 4). PAM05 has a very similar EOF modal decomposition (Figure 5), with a bipolar first modal structure explaining 61% of the variability and a tripolar second mode explaining 19.7% of the variability. The switch in order of importance of the tripolar and bipolar modes between the observations and the simulations is an indication that the simulated current vertical structure variability in the section is dominated by the passage of centered eddies through the channel. Interestingly, as in the observations both models agree with the surface confinement of the first mode and the deeper second mode.

To get some insight onto the causes of these two patterns of variability, present both in the observations and model simulations, Figure 6 shows the first two EOFs of CLIPPER ATL6 surface current anomalies around the Yucatan Channel. Mode 1 depicts a pattern with a marked shear oriented in the across-channel direction and could also be associated to the passage of eddies forced against the Cuban side of the channel; while mode 2 shows strong sheared flow in an along-channel direction and seems related to the passage of eddies more centered in the channel, or eddies that occupy most of the width of the channel. Mode 1 is related to the tripolar structure of the vertical section currents seen in Figure 4, as indicated by looking at its time evolution in the middle plot (thick line), where the time evolution of mode 2 from Figure 4 has been superposed (thin line). The correlation coefficient between these two series is 0.83. Similarly mode 2 of Figure 6 is associated with the bipolar structure observed in the modes of the vertical section in Figure 4. In this latter case the correlation coefficient between the two series is 0.95. This intimate relation between the principal modes of variability of the surface and vertical section current patterns is also confirmed by performing a “maximum covariance analysis” (*Storch and Frankignoul, 1998*) between the two fields. The results of this analysis (not shown) indicates that the patterns related to the bipolar mode account for 68 % and those related to the tripolar mode for 29 % of the co-varying fields.

### *Transports.*

Indicated in the previous section, the ATL6 and PAM05 simulated mean transport are larger than the observed 23.06 Sv 2-year mean. Actually, if the transport is calculated separately from the first (August/1999-June/2000) and second (July/2000-June/2001) period of observations, a transport of 23.0 and 23.2 Sv is obtained, respectively. Therefore the observed mean transport is very consistent between the two years of observations. Apart from this discrepancy in mean transport between the observations and model, there are other characteristics of the simulated transports’ structure and variability that will now be analyzed.

As mentioned above, there is a distinction from waters entering the Gulf through the Yucatan Channel above and below around 800 meters or the 6°C isotherm, since these are the maximum depth and the isotherm intersecting the bottom in the Strait of Florida at the section east of Miami, which can be considered as the exit of the Gulf of Mexico (*Niiler and Richardson, 1973, Bunge et al, 2002*). With this consideration in mind, when calculating transports through the Yucatan Channel, it is convenient to separate flows above and below this isotherm. The convention used here is that in the Yucatan Channel positive transports are into the Gulf of Mexico, while in the Strait of Florida section positive transports are out of the Gulf. Figure 7 shows time series of the observed total transport in Yucatan, along with the transport above and below the 6°C isotherm. Equivalent plots of transports for the 5-year CLIPPER ATL6 simulations are shown in Figure 8. Apart from the higher frequency content of the observed transport time-series due to different filtering for the observations and the CLIPPER data, the simulated transport series has a slightly higher variability for the total and above 6°C transports. The transports below the 6°C isotherm are similar in character for both the observations and the simulations, except that the mean differs, being -0.4 Sv into the Caribbean for the observations and 0.4 Sv into the Gulf for the simulations. These non-zero means for transports below 6°C are likely related to long-term oscillations (period of several years) of the deep water volume in the Gulf of Mexico as will be discussed later. The PAM05 3-year transport time series (Figure 9) simulations match well the magnitude of the observed variability for the total, above and below 6°C transports. However, the correlation coefficient between the simultaneous observed and simulated transports for any of the three series, is poor (~0.2). This will be looked at in more detail later when discussing the cross-spectra calculations.

An important discrepancy between the observed and simulated transport series is in the amplitude of their annual and semi-annual cycles. In the observations the through flow transport, related to transport above 6°C, has an annual cycle with an amplitude of only 0.2 Sv with maximum occurring in the middle of January. ATL6's through flow has an annual cycle with amplitude of 3.3 Sv with a maximum occurring the end of March and that of PAM05 has an annual cycle amplitude of 0.9 Sv with a maximum at the

beginning of March. The ATL6 annual cycle value coincides well with that reported for Yucatan by *Johns et al. (2002)* using the Naval Research Laboratory Atlantic basin model. The amplitude and phase of the semi-annual through flow transport in the observations is 1.1 Sv (larger than annual cycle), with a phase of  $-22^\circ$ , while that in ATL6 is 0.5 Sv and  $5^\circ$ , and in PAM05 is 0.1 Sv and  $-67^\circ$ .

Figures 10, 11 and 12 show the spectra and cross-spectra calculations between the transports above and below  $6^\circ\text{C}$  for the observations and the two simulations. Both in the observations and the simulations, transports in the two layers are quite incoherent (i.e. they do not show any significant correlation with each other) at all resolved frequencies, except for a peak at a period of around 17 days for ATL6 and around 21 days for PAM05, where they show a significant level of coherence. Actually, in the observations cross-spectrum, a relatively high (although not statistically significant) coherence peak is obtained at periods of around 18 days (Figure 10). In all three cases, observations, ATL6 and PAM05, these relatively high coherent peaks are associated with an  $180^\circ$  phase difference, and thus suggest a first baroclinic mode of motion between the transports in the two layers. This might be related to a first mode internal Kelvin wave propagating around the Gulf along the 800 m isobath. Considering that the perimeter of the 800 meter isobath in the Gulf of Mexico is  $3.9 \cdot 10^6$  m and that 20 days are  $1.73 \cdot 10^6$  s, such a wave would propagate at a phase speed of 2 to 3 m/s, which is quite reasonable according to the observed density structure.

As mentioned before the simulated PAM05 and observed transports, for the two years when they overlap, are very poorly correlated. This is also confirmed by calculating cross-spectra estimates, between the observed and simulated through flow transport, which show a lack of significant coherence at all resolved frequencies (Figure 13). The inability of the simulations to resemble the observed transport time evolution is expected considering that the region is dominated by meso-scale variability where instabilities processes are likely to occur frequently. Also, by not including the equatorial variability input, PAM05 is lacking an important component determining the evolution of the dynamics in the region. It is interesting, however, that the spectral profile of the through

flow for both observations and simulations are quite similar (Figure 13), indicating that the simulations are reproducing reasonably well the time scales involved (but not the phase).

In both simulations, the total transport time series at the section in the Strait of Florida (not shown) is perfectly correlated with that in the Yucatan Channel and, if calculated by layers it gives basically zero transport below 6°C. This is as expected due to the sill depth of the exit to the Gulf of Mexico.

To look in more details at the deep flows in and out of the Gulf of Mexico, Figure 14 gives the mean integrated transport below a given isotherm for the 2 years of observations in Yucatan Channel and for the 5-year simulation for the ATL6 sections in Florida and Yucatan. The observations give a mean zero transport below 7°C. However, if the calculation is done for each year separately (not shown) one obtains for the first year (Aug/99-June/00) a zero transport below 7.3°C, while for the second year (July/00-June/01) the zero transport is below 6°C. This can be interpreted as reflecting a long-period (several years) oscillation of the deep waters in the Gulf of Mexico, where at times the Gulf accumulates deep waters, raising its interface (~6°C) separating the upper and deep layers, while at others it drains them into the Caribbean Sea. This behavior is also reflected in the simulations. However, for the 5-year mean, the section in Florida gives zero transport below 5.5°C while the section in Yucatan gives positive transports for all the isotherms used. This could imply that the model has a strong vertical mixing in the Gulf or that 5 years is not long enough to complete a cycle of the deep water accumulation cycle. To look into this latter possibility in more detail, a calculation was performed using a 19-year simulation of the same CLIPPER ATL6 configuration but forced with a climatological “perpetual” year (including a seasonal cycle). In this specific climatological run there was no blocking of the eddy shedding by the Loop Current during the whole 19-year simulation. Figure 15 shows these calculations. Concentrating on the transports below 5°C the model shows no distinct long-term period of oscillation, and although there is appreciable energy present at periods of a year and longer, their variable phase prevents extracting a clear annual and/or several-year harmonic.

### *Eddy shedding by the Loop Current.*

In the 5-year CLIPPER ATL6 simulation studied here there were 6 eddies shed by the Loop Current. The shedding periods for these eddies were: one at 7, two at 8, two at 9 and one at 14 months. In the case of PAM05, in the 3-year simulation, there are 4 eddies shed with a time gap between shedding of 14, 8 and 10 months. In the two years of observations there were only two eddies shed (11/1999 and 4/2001), with an interval of 17 months between them. None of the PAM05's simulated eddy sheddings coincided with those observed. Even though both in the simulations and in observations the shedding period is not constant, ATL6 tends to favor a shedding period around 9 months (something verified in the 19-year climatological simulation), while in historical observations a 6-month shedding period is more frequent (*Sturges and Leben, 2000*). Although the dynamical mechanism for eddy shedding is not yet understood, it has been shown that the shedding is preceded by a decreased negative (anticyclonic) vorticity flux into the Gulf of Mexico through Yucatan Channel (*Candela et al., 2002*). Figure 16a shows the vorticity flux above 6°C in Yucatan calculated from the 5-year ATL6 simulation. The vorticity flux is calculated as:

$$\iint_{>6^{\circ}\text{C}} \frac{\partial v}{\partial x} \frac{\partial \rho}{\partial z} v dx dz ,$$

where  $v$  is the along channel current,  $x$  the cross-channel coordinate,  $z$  the vertical coordinate and  $\rho$  density. In the model this quantity is mostly negative throughout the five years, but has appreciable changes in intensity. Figure 16b shows the detrended time integration of the vorticity flux and the times of eddy shedding occurrence in the model indicated by the vertical shaded bars. As in the observations (*Candela et al., 2002*) it is noticed that the shedding of eddies by the Loop Current is consistently preceded by a decreased of negative vorticity flux into the Gulf of Mexico, which is related to a retraction of the Loop Current. Also, periods of increase negative vorticity flux cause the growth and extension of the Loop Current into the Gulf of Mexico. These two processes of growth and retraction related to the vorticity flux are clearly verified by analyzing animations of the surface current of the simulations together with the integrated vorticity flux time series.

In the case of PAM05 the vorticity flux calculations also confirm their relation to the shedding of eddies (Figure 17), however, it is not as clear as in the observations and in ATL6. In particular, on the 4 eddies shed in the PAM05 simulation, the one shed around February 2000 does not seem to be preceded by an immediate positive vorticity flux. Due to the higher horizontal resolution in PAM05 with respect to ATL6, the simulated flow reproduces smaller scale processes and therefore is prone to develop instabilities more readily. These aspects are clearly confirmed by analyzing animations of surface currents from both model configurations, where the PAM05 simulations show a more unstable and convoluted Loop Current than do those of ATL6. Consistently in the PAM05 animations it is seen that the instabilities in the Loop are triggered by abrupt changes in sign of the vorticity flux time evolution, something that should be looked into in more detail.

*Observed and modeled temperature and salinity fields in Yucatan Channel.*

The structure of the temperature and salinity fields simulated by the models in the Yucatan section are compared with the CTD surveys done during the CANEK cruises (Table I). Although the moored array recorded time series of temperature they did not reach to the surface and none recorded salinity. Therefore the comparisons of the temperature and salinity fields in Figures 18, 19 and 20 are qualitative in nature since the simulated 5-year for ATL6 and 3-year PAM05 time series are compared against 18 CTD survey realizations of the complete channel section during the cruises. Figure 18 shows the mean and standard deviation of the potential temperature in the channel. The mean potential temperature field is reasonably well simulated by both models in most of the section except for a lack of structure in the upper 100 meters and slightly colder than observed temperatures at the deepest part of the channel. The variability of the potential temperature field is also well reproduced by the simulations although both show a core of high variability at around 200 meters depth in the central part of the channel that is not present in the statistics of the CTD surveys.

The observed mean salinity section is also well simulated by ATL6 and PAM05 (Figure 19), except again for a lack of structure in the upper 100 meters, as was the case

in the potential temperature mean field. The relative maximum of salinity of the Subtropical Under Water at around 210 meters and the relative minimum of the Antarctic Intermediate Water at around 820 meters are well reproduced in both simulations. The simulated standard deviation of the salinity field has also high variability core at around 200 meters, which is not present in the observations, as was the case for the potential temperature field.

T-S diagrams of the observations and simulations compare well (Figure 20). However, both simulations give slightly smaller salinities ( $\sim 0.1$  PSU) for surface waters between 23 and 26 °C. In the deep layers, ATL6 separates the North Atlantic Deep Water into a distinct core and prolongs the salinity minimum characteristic of the Antarctic Intermediate Water, which in the channel is found at around 6°C, to temperatures less than 5°C. PAM05 seems to do a better representation of the deep waters characteristics, but we cannot conclude that it is an effect of the higher resolution. Indeed, this is more likely a consequence of the model configuration: model T and S are strongly relaxed to observed climatological values at the southern boundary at 9°N, which certainly has an effect on the apparent better conservation of T, S properties in the Caribbean and the Yucatan Channel. Also both simulations have stronger mixing in the upper surface layer compare to reality, which is reflected in the deep surface mixed layer in the temperature and salinity plots and in the upper part of the T-S diagram.

## ***5 Discussions and Summary***

The purpose of this study has been to investigate the dynamics of the Yucatan Channel both with observations and with the CLIPPER-ATL6 and MERCATOR-PAM05 model configurations (both using the OPA ocean general circulation numerical code). In particular, there has been a detailed comparison of the simulation performance against a two-year observation period of the flows through Yucatan Channel by the CANEK measuring Program. From the CANEK Program we have now a good idea of the structure of flows in Yucatan. The 2-year mean total transport of 23.06 Sv observed in Yucatan differs from ATL6's 27.48 Sv, PAM05's 29.06 Sv and from the commonly

accepted value of 28 Sv deduced from historical hydrographic observations or from recent measurements of the inflow through the Lesser Antilles passages and modeling efforts (*Schmitz and McCartney, 1993; Johns et al, 2002*). However, due to the high degree of variability of the flows in and out of the Caribbean and Gulf of Mexico, solving this discrepancy requires a large observational effort were all the entrances to the system are monitored simultaneously. Both model configurations use a “free slip” lateral boundary conditions, which might favor stronger transports. In the case of the ATL6 simulations, overestimating the flows through Yucatan might also be linked to an observed mean circulation around Cuba where the water leaving the Gulf of Mexico flow along the northern Cuban coast and reenter the Caribbean through Windward Passage.

The observed current structure in the Channel section is dominated by two principal modes as revealed by an EOF decomposition: one with a tripolar structure with coherent currents on the Yucatan and Cuban sides and opposing currents at the center of the channel, and another with a bipolar structure with opposing currents on both sides (*Abascal et al., 2003*). These two modal structures are well reproduced by the ATL6 and PAM05 simulations. In the latter case, the lack of meso-scale variability of equatorial origin does not seem to have a negative effect on its ability to reproduce the observed current structure variability in the Yucatan Channel’s section.

In the two years of observations the transports in Yucatan do not show a clear annual cycle, while ATL6 has one with an amplitude of 3.3 Sv. This is also observed in other models (*Johns et al, 2002*). In the observations, although there is appreciable energy present in the transports at the annual period, its phase is quite variable and therefore a clear annual harmonic is hardly resolved from the two-year time series. A similar behavior is shown in the PAM05 simulations that do not have an appreciable annual cycle and resemble better the observed transports in this aspect.

From the observations-model comparison it is evident that it is required to look in more detail the model’s vertical mixing, which seems too high. A possibility for this to happen is a numerically induced diapycnal mixing due to z-level coordinates and the use

of hyper viscosity as sub-grid-scale parameterization. However, in other aspects it has been found (*Barnier et al, 2001*) that one of the models' deficiencies is the lack of enough vertical penetration of eddy kinetic energy.

When looking at the observed vertical temperature and salinity structures in the channel and comparing them with those in the simulations it is clear that the model is over-mixing the surface upper 100 meters unrealistically reducing the observed surface stratification. Also when comparing observed and modeled T-S diagrams indications of excessive mixing at depth are also present. In particular the ATL6 simulations show that the low salinity core of the Intermediate Antarctic Water is over-mixed with the underlying North Atlantic Deep Water, which is not present in the PAM05 simulations, likely due to the proximity of the southern boundary relaxation zone in that configuration.

Both simulations confirm that the eddy shedding by the Loop current is preceded by a period of diminish negative horizontal vorticity flux into the Gulf of Mexico, something which has been well documented happening in the observations (*Candela et al, 2002*). In the case of the PAM05 simulations, its higher horizontal resolution enhances the onset of instabilities in the Loop Current more readily than in ATL6, and these seem to be playing a major role in the eddy shedding events. Recently, in a regional model study of the Gulf of Mexico and Caribbean, *Ezer et al (2003)* related the eddy shedding events to variability in the transport intensity of the Yucatan Current. Another numerical study (*Oey and Lee, 2002*) also indicates that irregular shedding occurs as a result of fluctuating Yucatan Current transports forced by variable winds over the region. However, in both of these studies the transport variability is not related to changes in horizontal vorticity flux, which in reality are likely to be correlated. *Pichevin and Nof (1997)* have proposed a theory for the shedding of eddies by the Loop Current based on what they termed "the momentum imbalanced paradox". This theory implies that a light current exiting from a channel perpendicular to the coastline, exerts a flow-force parallel to the coast wall, which cannot be balanced without the generation of eddies on the opposite side. The theory predicts a reasonable eddy shedding behavior for the Loop Current, but its relation to the vorticity flux conditions at the prescribed coastal inflow

have not been investigated as to permit a detailed comparison with the results present here.

Both ATL6 and PAM05 are reliable model configurations that can be used in the region to understand some dynamical aspects of the observed flow field. Considering that in the case of ATL6 the domain is the whole Atlantic Ocean, its good behavior in the Yucatan Channel region speaks highly of its overall reliable performance. In the PAM05 configuration it is interesting to observe that the main time scales of the observed variability in the channel are well reproduced even though its domain does not include the equatorial region (and thus has no North Brazil Current eddies entering the Caribbean Sea). As both simulations agree with the observations well, they can be used to study in more detail the spatial structure and variability of the processes in the Yucatan Channel and the Gulf of Mexico complementing the observations in the study of the regional dynamics.

From analyzing the ATL6 and PAM05 simulations and based on previous results and those presented here, there seems to be a strong indication that in order to reproduce the time evolution of processes in the Yucatan Channel, and in the Gulf of Mexico-Caribbean Sea system in general, is it required to include the equatorial dynamics in the model configuration (*Murphy et al, 1999; Johns et al, 2002*). However, other models that do not include the equatorial variability explicitly (*Ezer et al, 2002*) are also able to reproduce a large part of the observed current structure in Yucatan, as shown by the PAM05 simulations reported here. If the objective of the model being developed is to be eventually used in a data assimilation scheme, as long as the model is reproducing the dynamics correctly this issue might not be important, but to understand how much of the observed variability is locally vs. remotely forced, clearly requires further research using models without data assimilation and which include explicitly the variability generated in the equatorial region.

## References

- Abascal A., J. Sheinbaum, J. Candela, J. Ochoa and A. Badan, Structure and variability of the flow in the Yucatan Channel, *Journal of Physical Oceanography*, submitted.
- Andrade, C.A. and E.D. Barton, Eddy development and motion in the Caribbean Sea. *Journal of Geophysical Research*, 105 (C11), 26,191-26,201, 2001.
- Barnier, B., T. Reynaud, A. Beckman, C. Böning, J-M Molines, S. Barnard and Y. Jia, On the seasonal variability and eddies in the North Brazil Current: insights from model inter-comparison experiments, *Progress in Oceanography*, 48, 195-230, 2001.
- Bunge, L., J. Ochoa, A. Badan, J. Candela and J. Sheinbaum, Deep flows in the Yucatan Channel and their relation to changes in the Loop Current extension. *Journal of Geophysical Research*, in press.
- Candela, J., J. Sheinbaum, J. Ochoa, A. Badan and R. Leben, The potential vorticity flux through the Yucatan Channel and the Loop Current in the Gulf of Mexico. *Geophysical Research Letters*, 29(22), 10.1029/2002GLO15587, 2002.
- Ezer, T., L-Y Oey and H-C Lee, The variability of currents in the Yucatan Channel: Analysis of results from a numerical ocean model, *Journal of Geophysical Research*, in press.
- Gibson, et al, 1997.
- Madec G., P. Delecluse, M. Imbard and C. Levy, Ocean General Circulation Model reference manual. *Note du Pôle de modélisation*, Institut Pierre-Simon Laplace (IPSL), France, N°XX, 91pp., 1999.
- Murphy S.J., H.E. Hurlburt and J.J. O'Brien, The connectivity of eddy variability in the Caribbean Sea the Gulf of Mexico and the Atlantic Ocean, *J. Geophys. Res.*, 98 (C1), 1431-1453, 1999.
- Mooers, C.N.K. and G.A. Maul, Intra-Americas Sea circulation. In: *The Global Coastal Ocean/Regional Studies and Synthesis*, (ed. K.H. Brink and A.R. Robinson), *The Sea*, 11, John Wiley, New York, 140-157, 1998.
- Niiler, P.P. and W.S. Richardson, Seasonal variability of the Florida Current, *J. Mar. Res.* 31, 144-167, 1973.
- Ochoa J., J. Sheinbaum, A. Badan, J. Candela and D. Wilson, Geostrophy via potential vorticity inversion in the Yucatan Channel. *Journal of Marine Research*, Vol. 59, 725-747, 2001.
- Oey, L.-Y. and H.-C. Lee, External forcings that influence the irregular eddy shedding from the Loop Current, Submitted, 2002.
- Johns, W.E., T.L. Townsend, D.M. Frantantoni and W.D. Wilson, On the Atlantic inflow to the Caribbean, *Deep-Sea Res.*, I, 49, 211-243, 2002.
- Pichevin, T. and D. Nof, The momentum imbalance paradox, *Tellus*, 49 A, 298-319, 1997.

- Reynaud T., P. Legrand, H. Mercier and B. Barnier, A new analysis of hydrographic data in the Atlantic and its application to an inverse modeling study, *International WOCE Newsletter*, Number 32, 29-31, 1998.
- Schmitz, W. J., Jr. and M.S. McCartney, On the North Atlantic circulation. *Rev. Geophys.* 31, 29-49, 1993.
- Sheinbaum, J, J. Candela, A.Badan and J. Ochoa, Flow structure and transport in Yucatan Channel. *Geophysical Research Letters*, 29(3), 10.1029/2001GL013990, 2002.
- Sheng, J. and L. Tang, A numerical study of circulation in the western Caribbean Sea, *J. Phys. Oceanogr.*, in press.
- Smith W.H.F. and D.T. Sandwell, Global Seafloor topography from satellite Altimetry and ship depth soundings, *Science*, 277, 1956-1962, 1997.
- Sturges W. and R. Leben, Frequency of ring separation from the Loop Current in the Gulf of Mexico: A revised estimate. *J. Phys. Oceanogr.*, 30, 1814-1819, 2000.
- Treguier A-M, B. Barnier, A. de Miranda, J-M. Molines, N. Grima, M. Imbard, G. Madec, C. Messenger and S. Michel, An eddy permitting model of the Atlantic circulation: evaluating open boundary conditions, *Journal of Geophysical Research*, 2001, in press.
- von Storch, H. and C. Frankignoul, Empirical modal decomposition in coastal oceanography, *The Sea*, Volume 10, ed. K. H. Brink and A. R. Robinson, John Wiley & Sons Inc., 419-455, 1998.

Cruise	Period	Number of sections
Canek 0	7 to 18 December, 1996	No complete sections
Canek 1	24 May to 12 June, 1997	3
Canek 2	29 March to 6 April, 1998	3
Canek 3	27 January to 6 February, 1999	2
Canek 4	25 August to 14 September, 1999	4
Canek 5	16 June to 10 July, 2000	4
Canek 6	20 June to 6 July, 2001	3
Canek 7	16 August to 2 September, 2002	1

Table 1. Cruises done during the Canek Program indicating the cruise period and the number of complete CTD sections across Yucatan Channel done in each cruise.

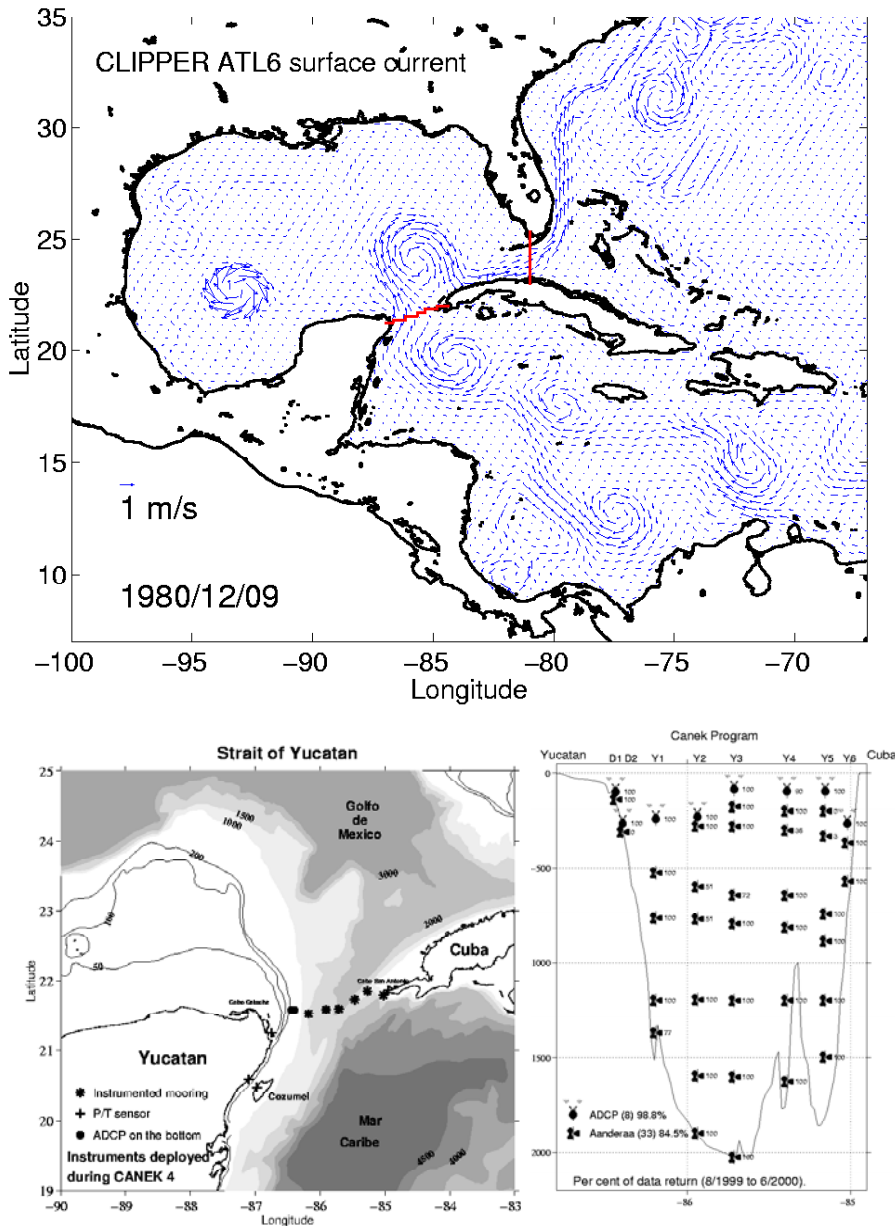


Figure 1. The upper plot is a map of the Gulf of Mexico and western part of the Caribbean Sea showing the simulated surface currents for December 9, 1980 by the CLIPPER ATL6 Model and indicating the sections where modeled data was extracted in the Yucatan Channel and Florida Straits to compare with observations. The lower left plot gives the position of the moorings in the Yucatan Channel and in the lower right the instrument layout in the water column. These moorings were maintained for 23 months (Aug./1999-June/2001) as part of the CANEK Program.

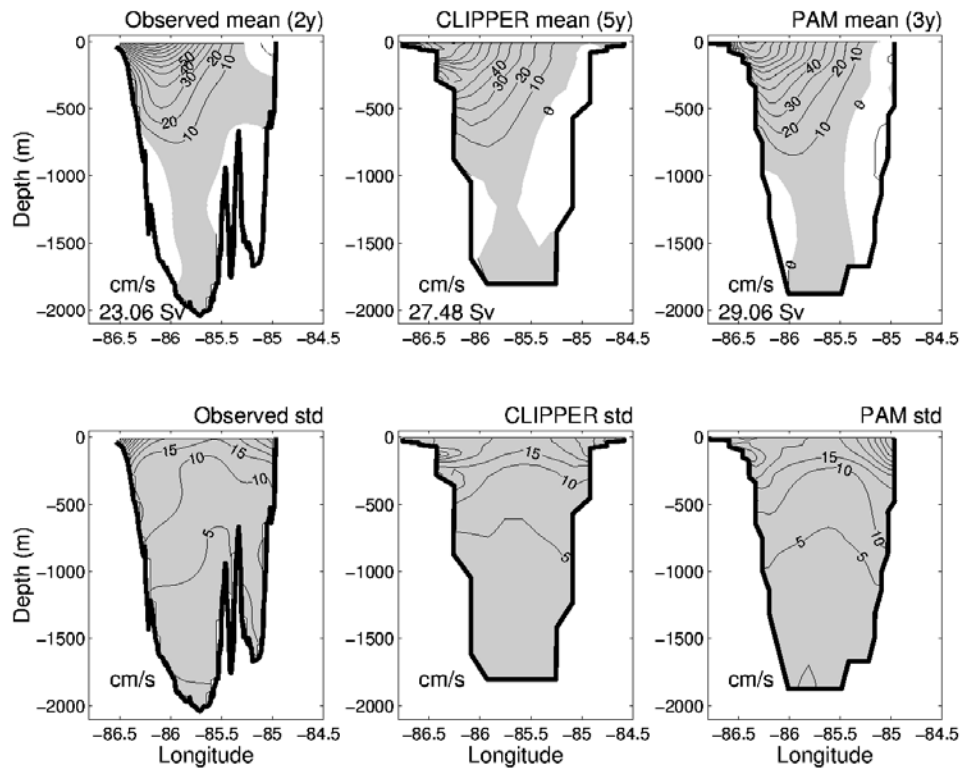


Figure 2. Structure and variability of the along-channel current in Yucatan Channel's main section based on two years of observations during the Canek Program (left panels), 5 years of CLIPPER ATL6 simulations (central panels) and 3 years of MERCATOR PAM05 simulations (right panels).

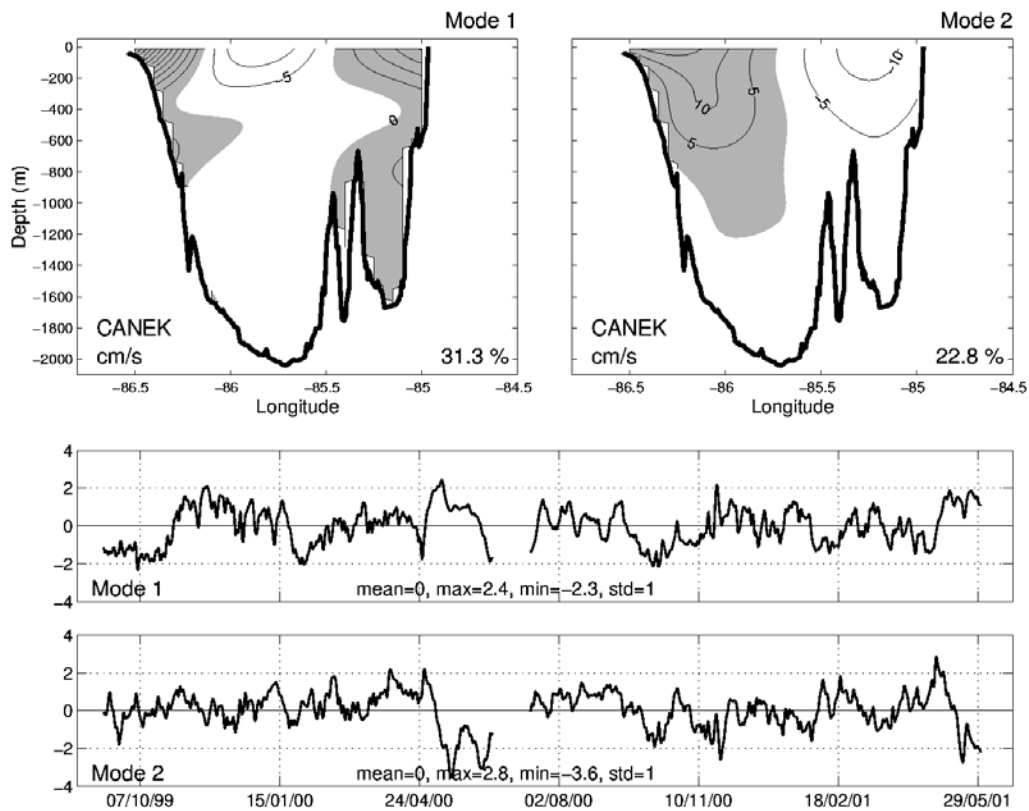


Figure 3. First two EOFs of the along-channel current in Yucatan based on two years of observations. The modal spatial structure (upper panels) and their time evolution (lower panels) are shown.

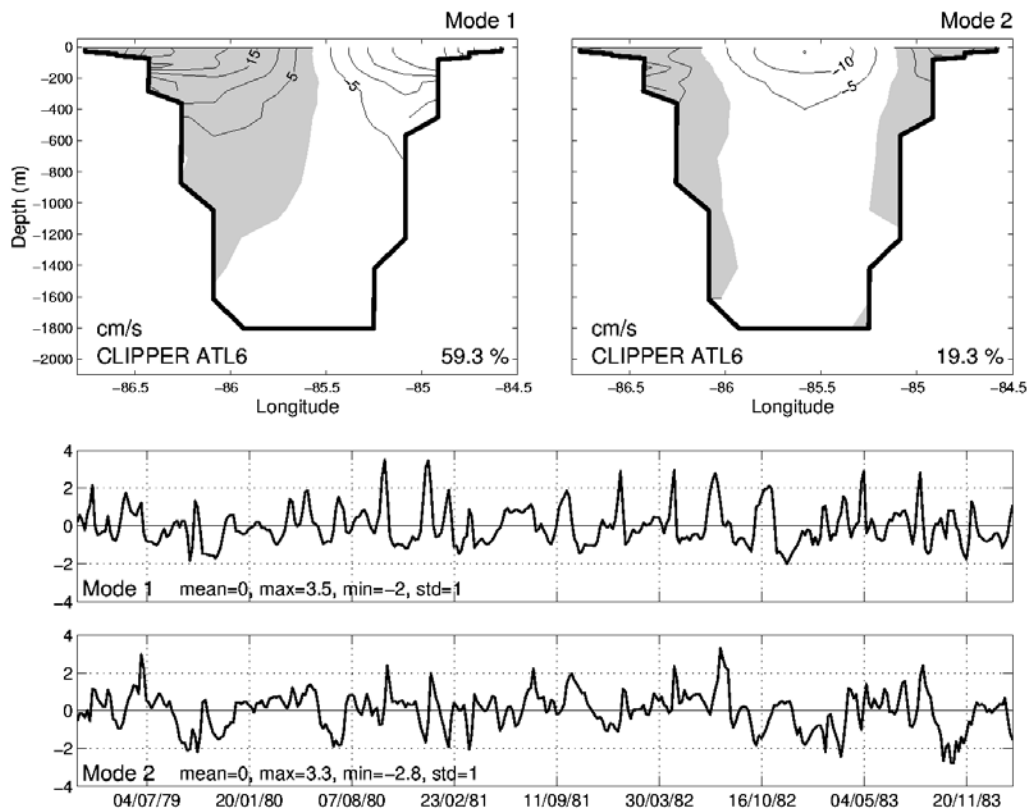


Figure 4. First two EOFs of the along-channel current in Yucatan based on 5 years of simulation using the CLIPPER ATL6 model. The modal spatial structure (upper panels) and their time evolution (lower panels) are shown.

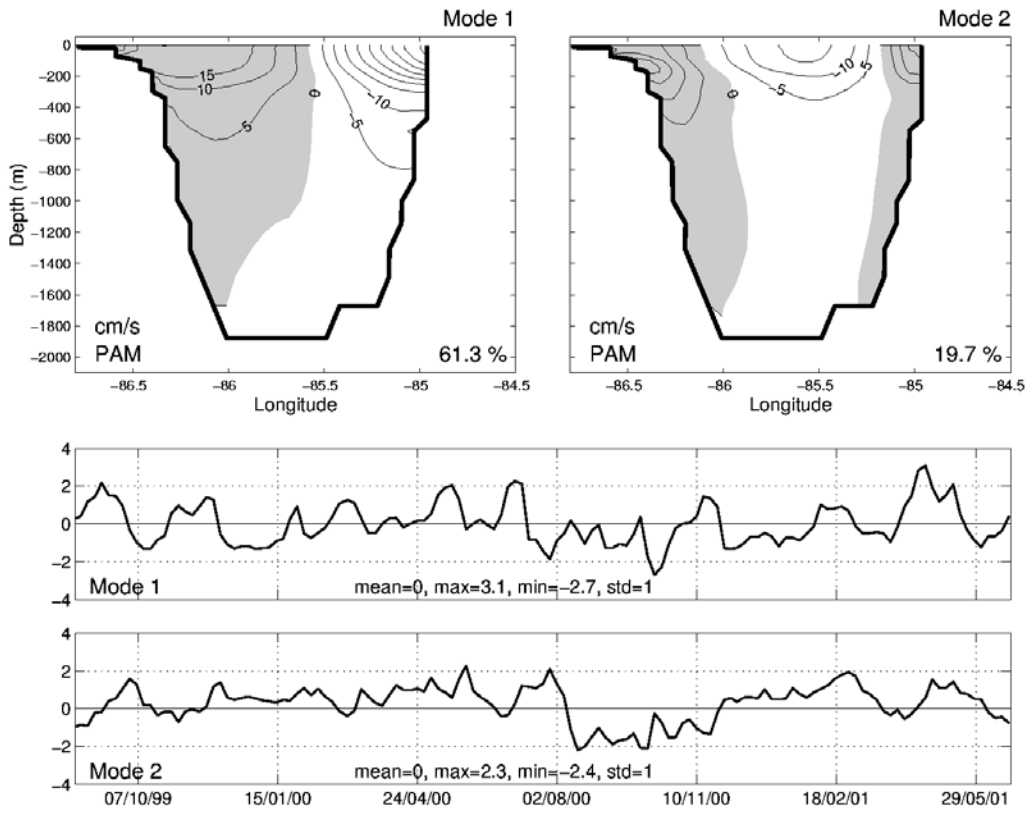


Figure 5. First two EOFs of the along-channel current in Yucatan based on 3 years of simulation using the PAM05 model. The modal spatial structure (upper panels) and their time evolution (lower panels) are shown.

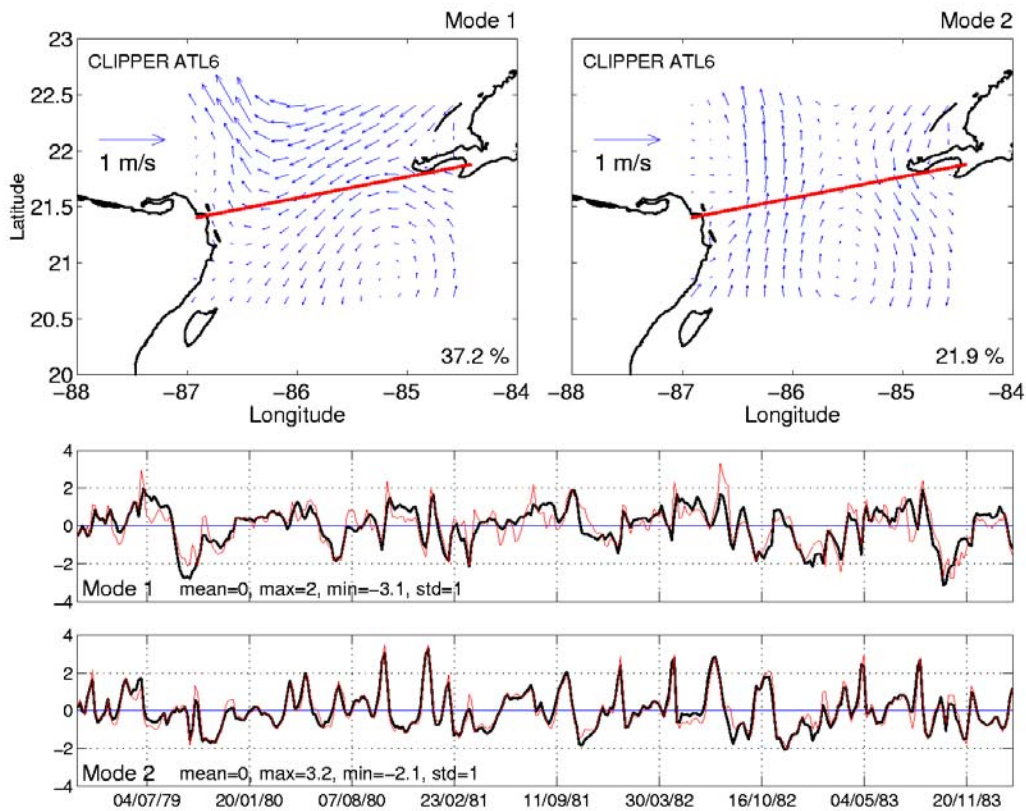


Figure 6. First two EOFs of the CLIPPER ATL6 Model simulated surface currents anomalies around the Yucatan Channel. The upper two panels show the spatial current patterns related to the first two modes and the line across the channel indicates the section that was used to calculate the vertical patterns calculated in Figure 4. The time evolution of each mode is shown in the lower two panels by the thick line. The thin line in the plot for mode 1 corresponds to the time evolution of mode 2 from Figure 4 of the vertical section EOFs and that in the plot for mode 2 to mode 1 of Figure 4 (see text for explanation).

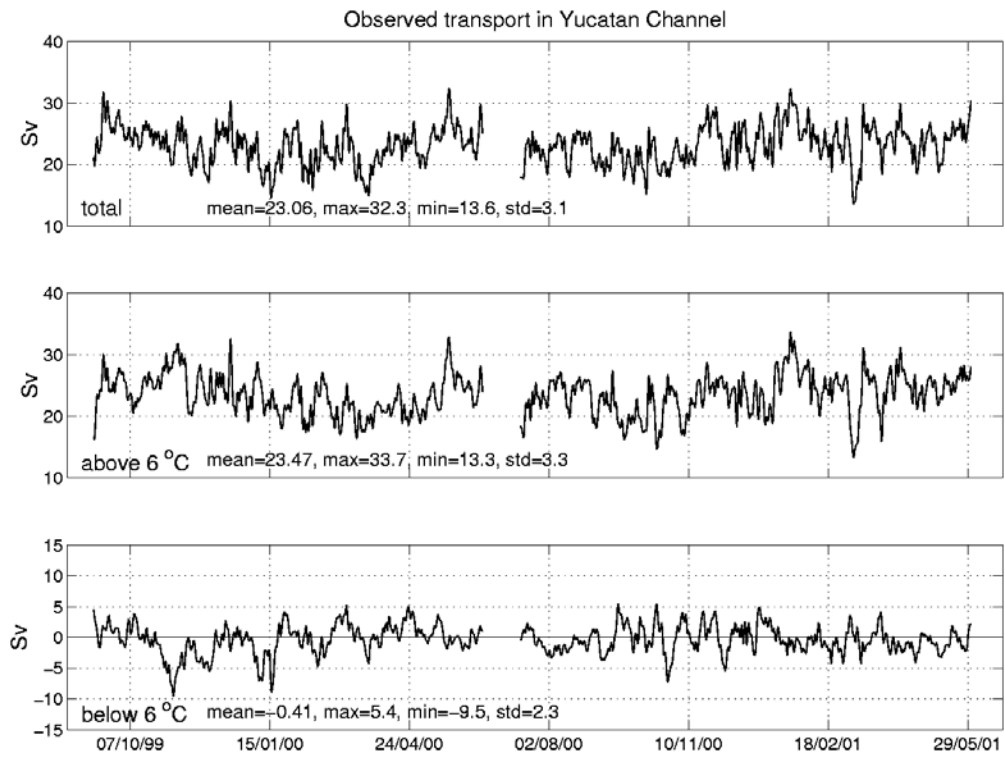


Figure 7. Time series of the observed transport in the Yucatan Channel. The total (upper panel), above the 6°C isotherm (middle panel) and below the 6°C isotherm (lower panel) transports are shown for the period between August 1999 to June 2001.

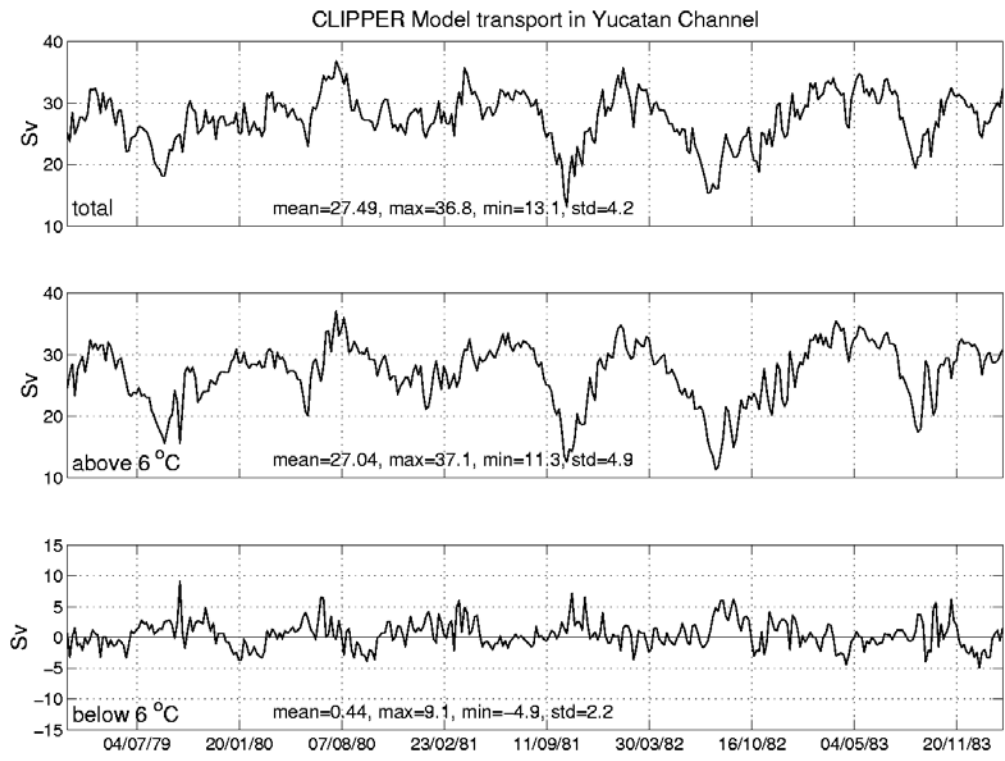


Figure 8. Time series of CLIPPER ATL6 model simulated transport in the Yucatan Channel. The total (upper panel), above the 6°C isotherm (middle panel) and below the 6°C isotherm (lower panel) transports are shown.

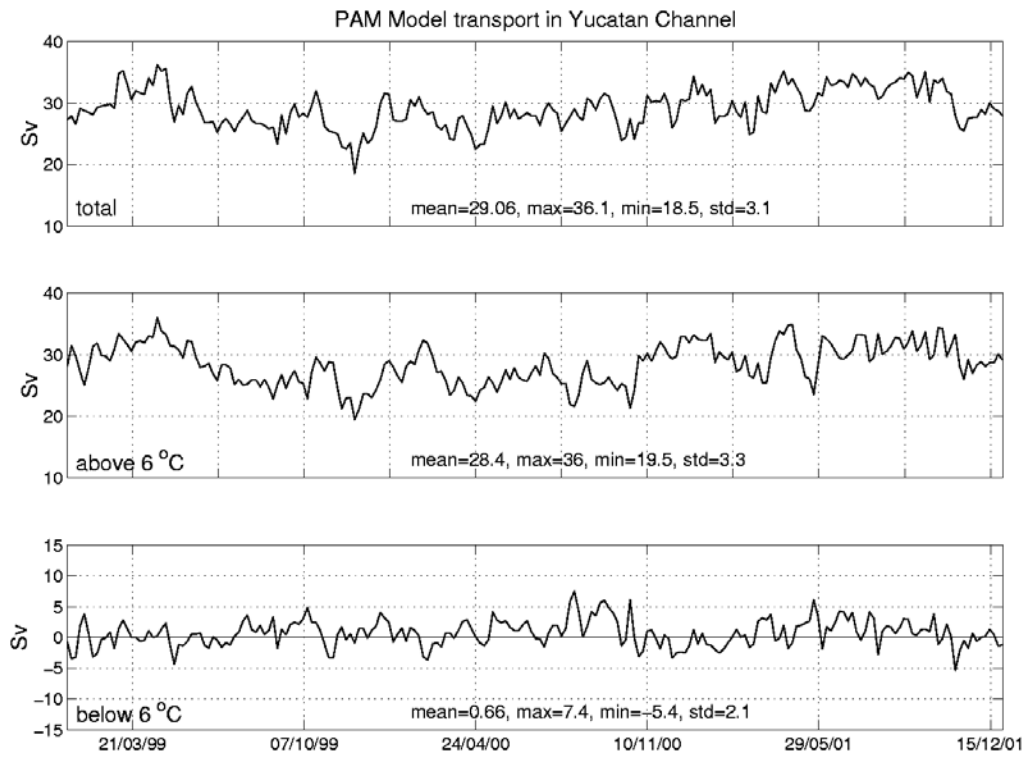


Figure 9. Time series of PAM05 model simulated transport in the Yucatan Channel. The total (upper panel), above the 6°C isotherm (middle panel) and below the 6°C isotherm (lower panel) transports are shown.

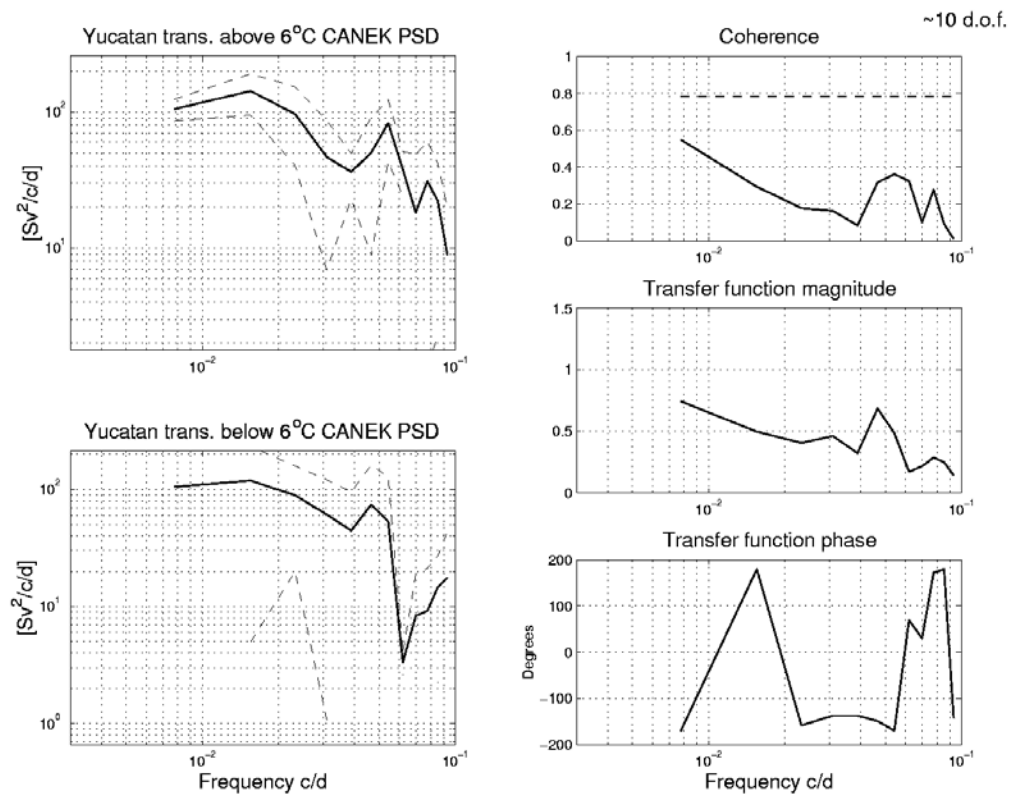


Figure 10. Spectra and cross-spectra of the observed transports in the Yucatan Channel above and below the 6°C isotherm shown in Figure 7.

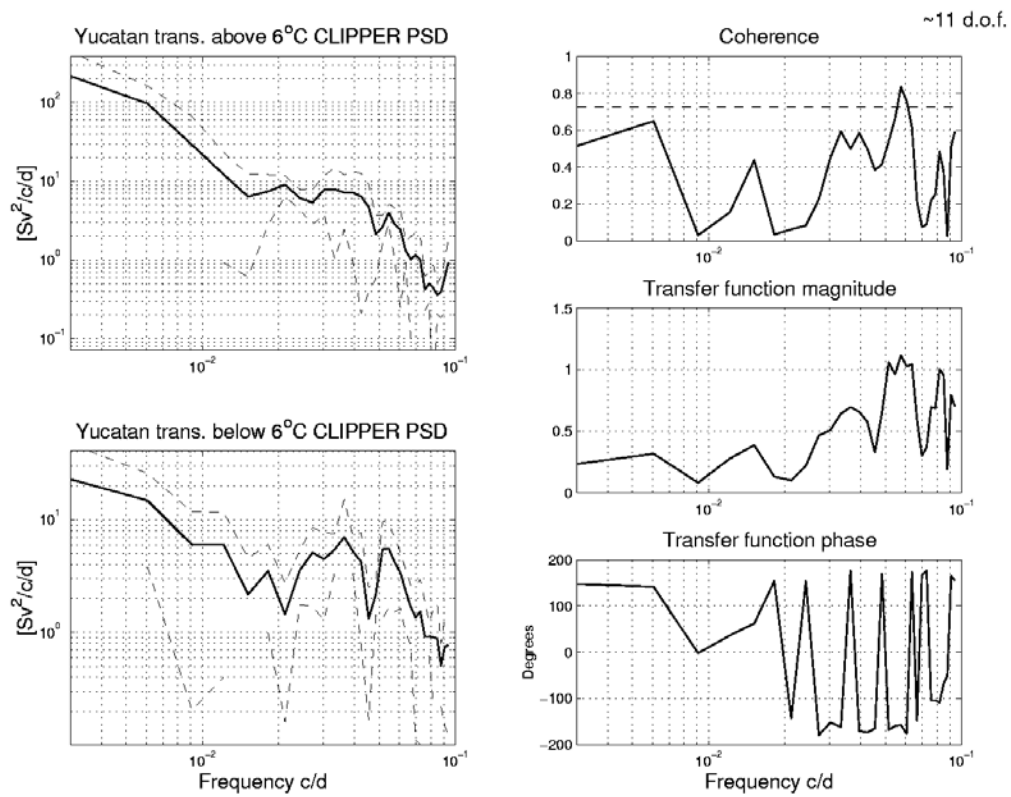


Figure 11. Spectra and cross-spectra of the CLIPPER ATL6 simulated transports in the Yucatan Channel above and below the 6°C isotherm shown in Figure 8.

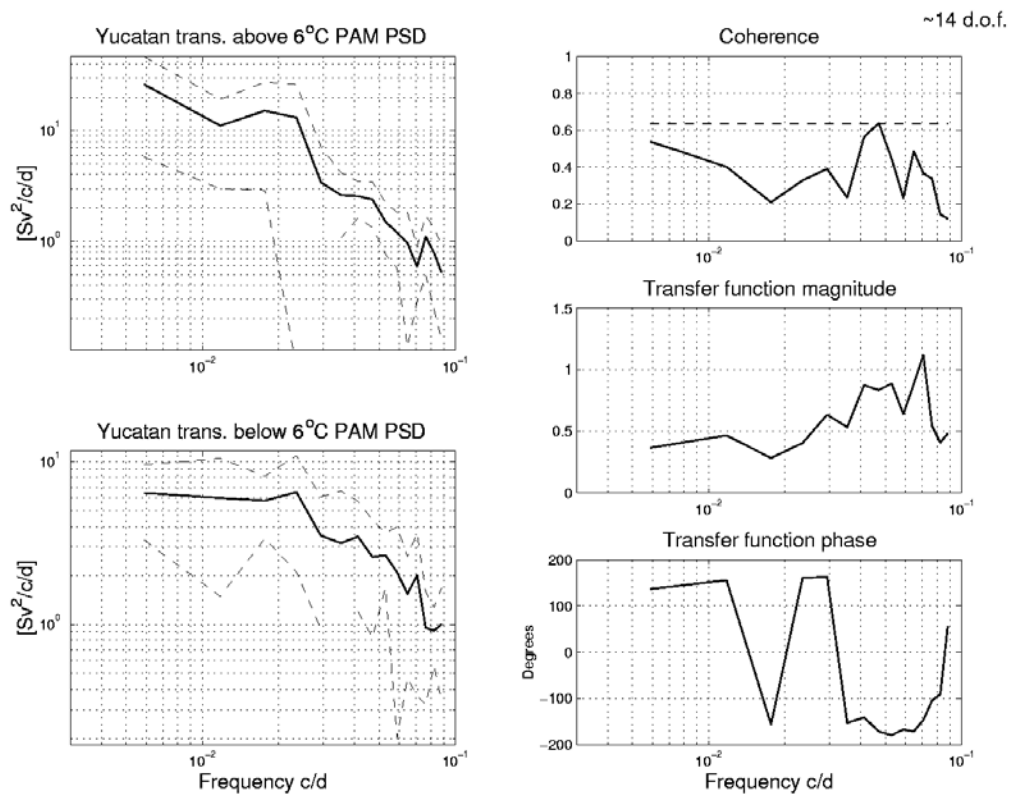


Figure 12. Spectra and cross-spectra of the MERCATOR PAM05 simulated transports in the Yucatan Channel above and below the 6°C isotherm shown in Figure 9.

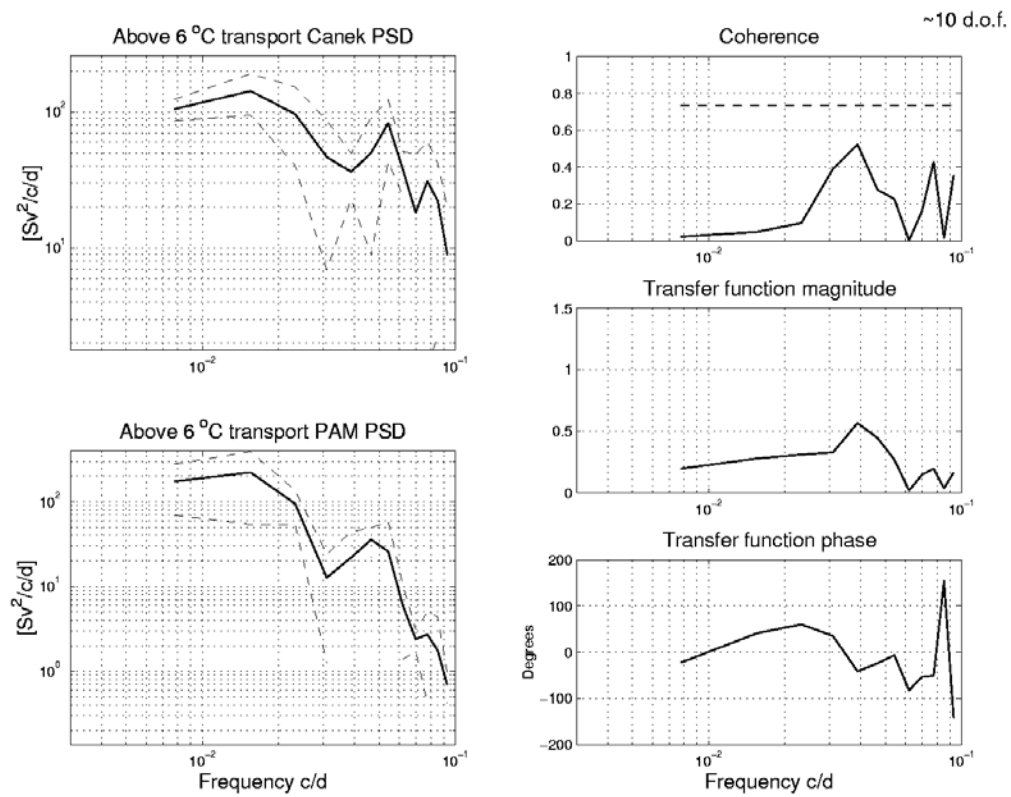


Figure 13. Spectra and cross-spectra of the observed and PAM05 model simulated transports in the Yucatan Channel above the 6°C isotherm for the two-year period when both series overlap.

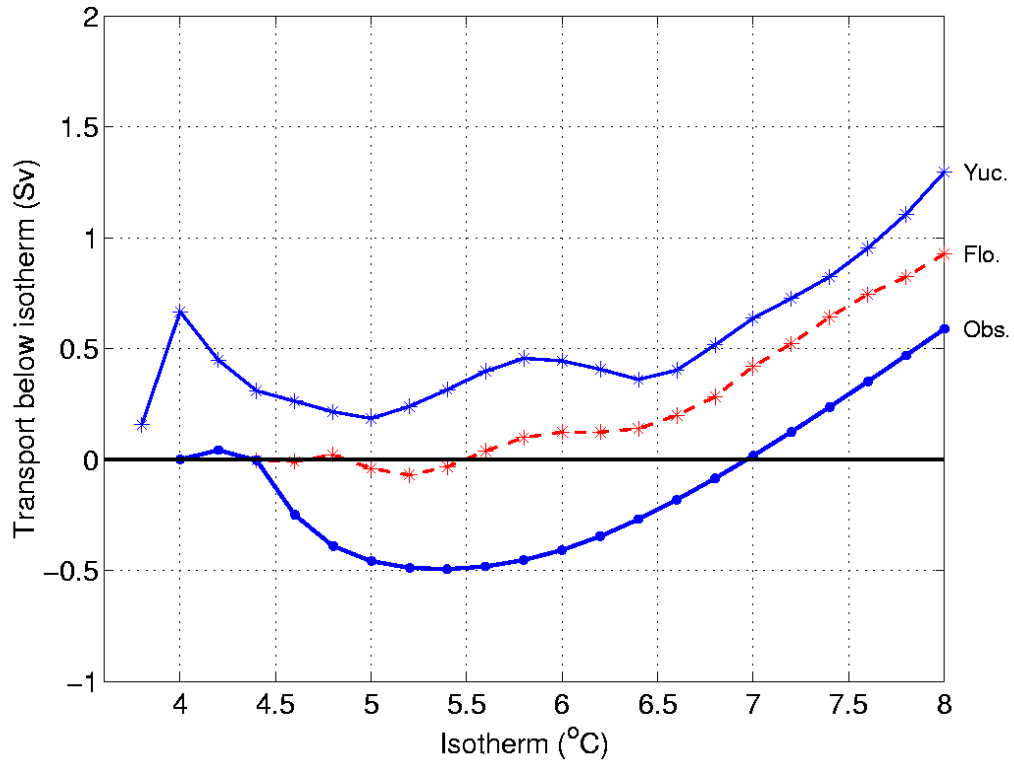


Figure 14. Mean transports below a given isotherm. Curves for the observed 2-year transports in the Yucatan Channel during the Canek Program (Obs.), for those simulated by the CLIPPER ATL6 Model for the period 1979-1983 in Yucatan (Yuc.) and the Strait of Florida (Flo.).

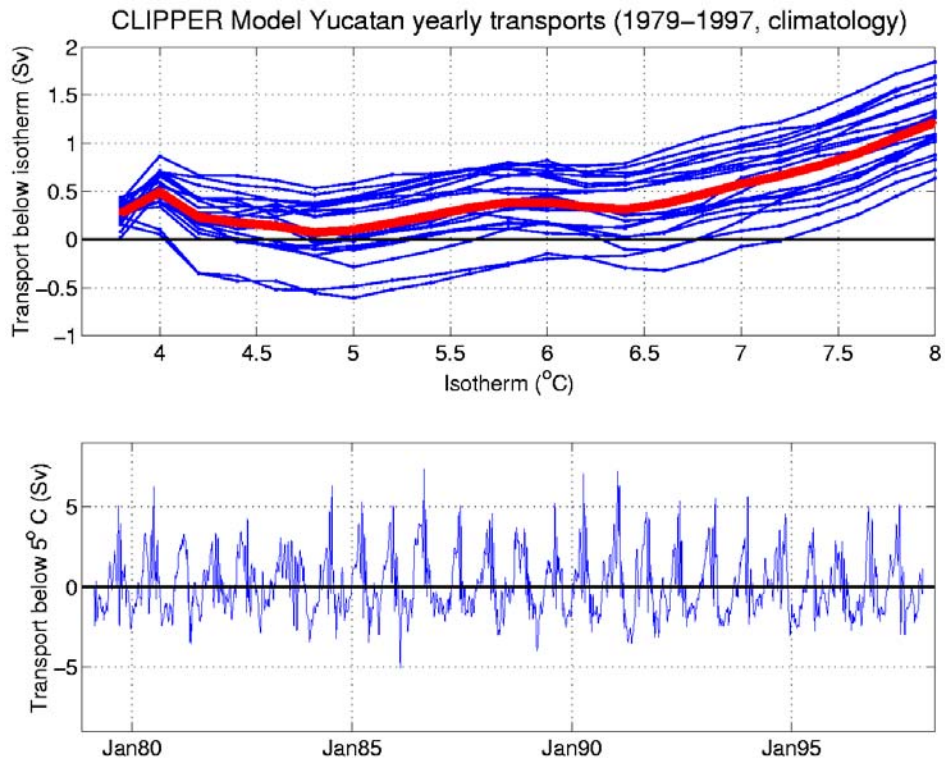


Figure 15. Yearly transports in Yucatan Channel below a given isotherm from the CLIPPER model when forced by a climatological mean year for 19 years (upper plot). The thick line in the plot corresponds to the mean transport over the 19 years. Time series of the transport in Yucatan Channel below 5°C from the CLIPPER model forced with climatology (lower plot).

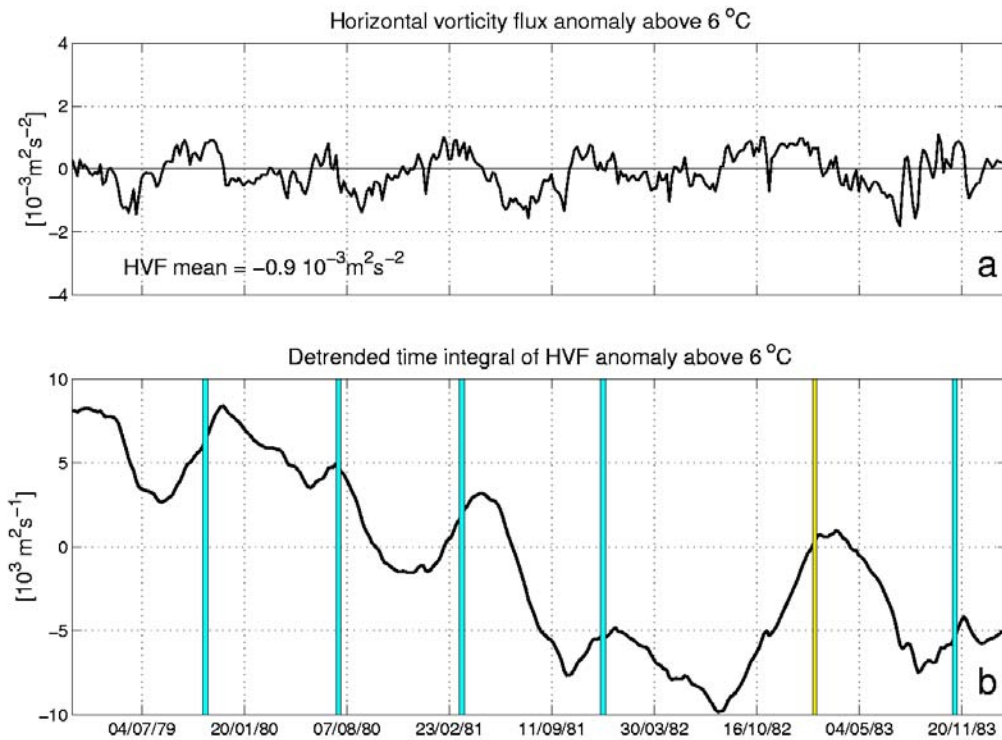


Figure 16. CLIPPER ATL6 Model simulation of the vorticity flux anomaly due to the horizontal shear through the Yucatan Channel above the 6 °C isotherm (a). Detrended time integral of the vorticity flux (b). Also indicated in this plot are the times when eddies were shed by the Loop Current in the model (vertical bars).

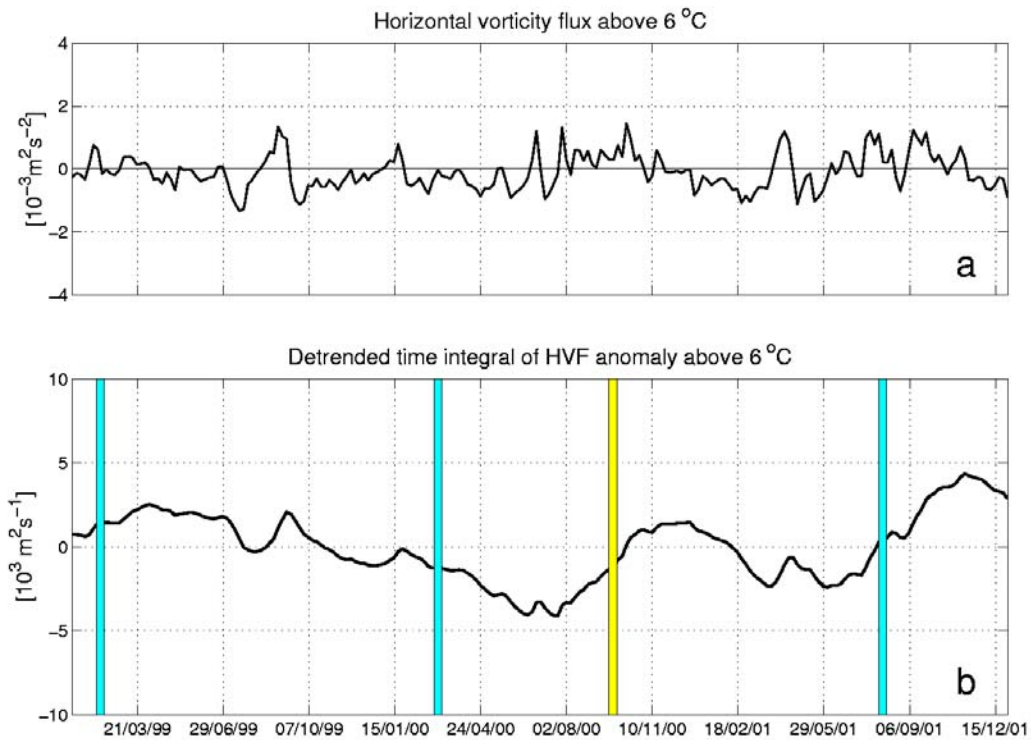


Figure 17. PAM05 simulation of the vorticity flux due to the horizontal shear through the Yucatan Channel above the 6 °C isotherm (a). Detrended time integral of the vorticity flux (b). Also indicated in this plot are the times when eddies were shed by the Loop Current in the model (vertical bars).

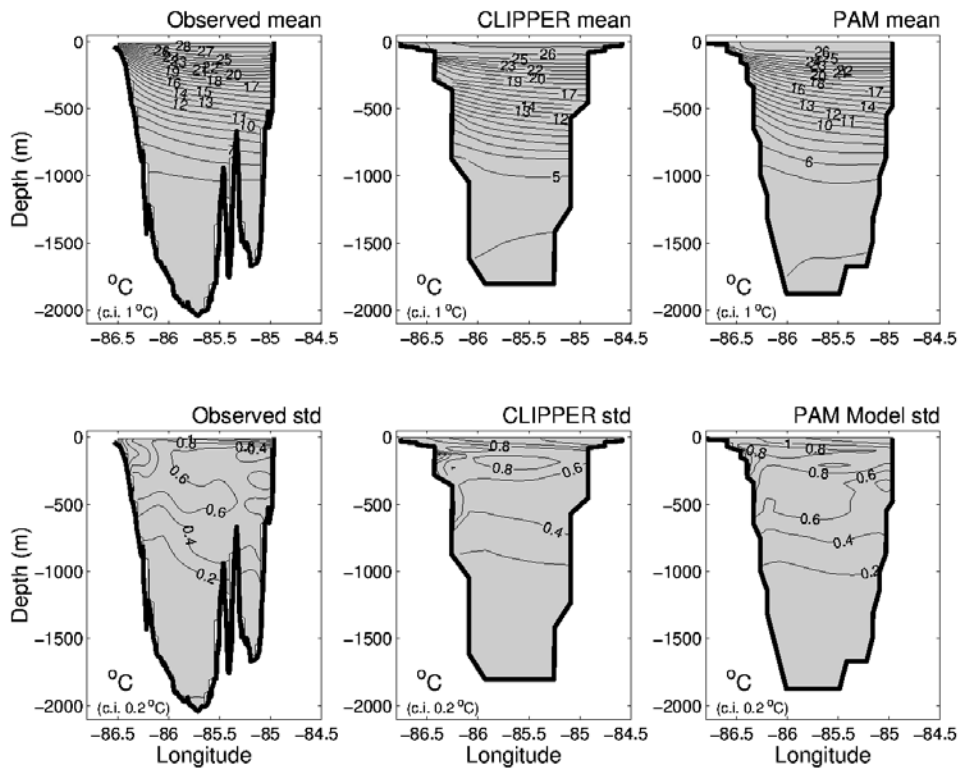


Figure 18. Structure and variability of potential temperature in Yucatan Channel’s main section based on 18 CTD sections obtained during the Canek Program (left panels), 5 years of CLIPPER ATL6 simulations (central panels) and 3 years of PAM05 simulations (right panels).

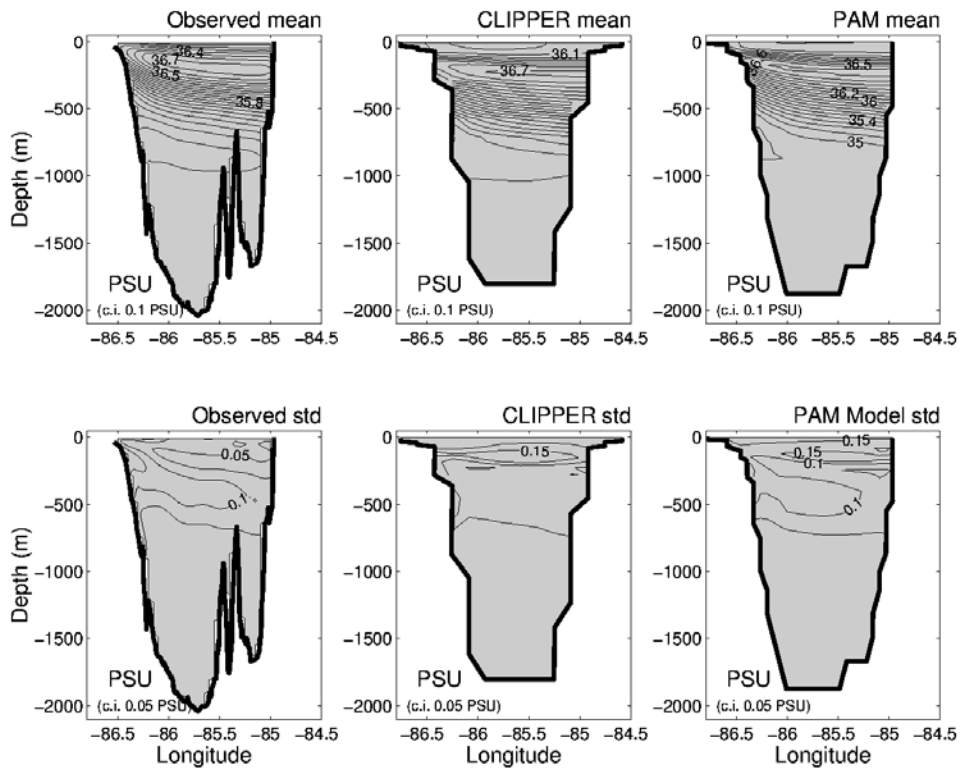


Figure 19. Structure and variability of salinity in Yucatan Channel’s main section based on 18 CTD sections obtained during the Canek Program (left panels), 5 years of CLIPPER ATL6 simulations (central panels) and 3 years of MERCATOR PAM05 simulations (right panels).

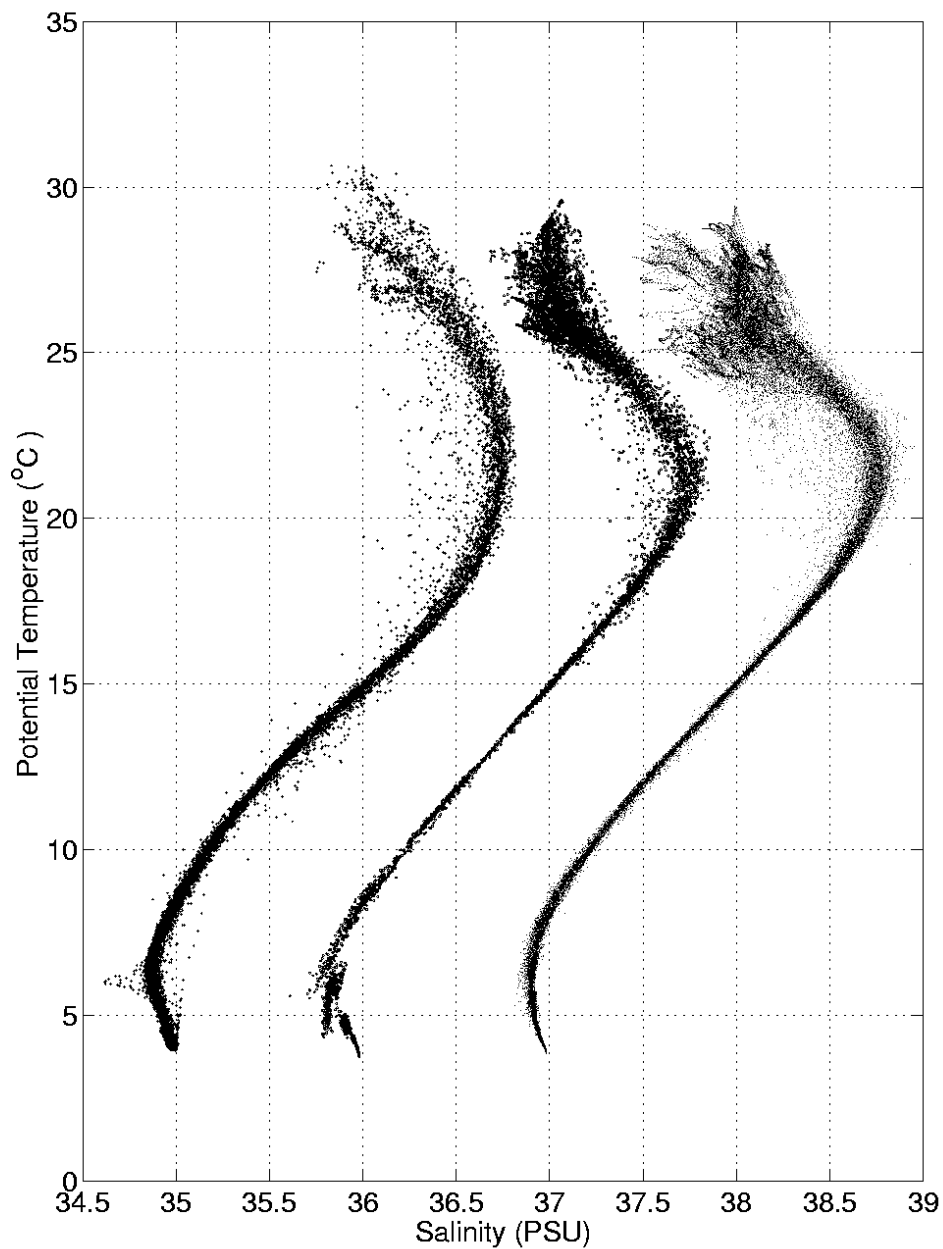


Figure 20. T-S diagram for Yucatan Channel's main section based on 18 CTD sections obtained during the Canek Program (+ signs, right curve), 5 years of CLIPPER ATL6 simulations (small circles, central curve) and 3 years of PAM05 simulations (dots, right curve). The T-S curves for the model simulations have been displaced by +1 PSU for ATL6 and +2 PSU for PAM05, for clarity.